

An Integrated Deep Learning Framework Enables Rapid Spatiotemporal Morphodynamic Predictions Toward Long-Term Simulations

5 Mohamed M. Fathi^{1,2}, Zihan Liu³, Anjali M. Fernandes⁴, Michael T. Hren⁵, Dennis O. Terry, Jr.⁶, C. Nataraj³, and Virginia Smith⁷

¹ Dept. of Civil Engineering, Florida Gulf Coast University, United States;

10 ² Dept. of Civil Engineering, Faculty of Engineering, Fayoum University, Egypt;

³ Villanova Center for Analytics of Dynamic Systems and Department of Mechanical Engineering, Villanova University, United States;

⁴ Dept. of Earth and Environmental Sciences, Denison University, United States;

⁵ Dept. of Earth Sciences, University of Connecticut, United States;

15 ⁶ Dept. of Earth and Environmental Science, Temple University, United States;

⁷ Dept. of Civil and Environmental Engineering, Villanova University, United States.

Correspondence to: Mohamed M. Fathi (m.fathi.said0@gmail.com & msaid@fgcu.edu)

20

Abstract

Physics-based morphodynamic modeling is essential for advancing river management science and understanding Earth's geomorphological evolution processes. However, their computational demands and long processing times hinder long-term applications. This paper introduces and tests a robust Deep Learning (DL) framework that opens the door to overcoming these challenges through integrating convolutional neural networks (CNNs) with long short-term memory (LSTM) architectures, trained using outputs from the physics-based HEC-RAS model. This framework facilitates rapid and continuous spatiotemporal predictions of hydrodynamic parameters and morphodynamic responses of flood events. Hydrodynamic predictions showed strong performance across the testing dataset, with mean RMSEs of 0.15 m and 0.04 m/s for water depth and flow velocity, respectively. Bed change predictions also demonstrated promising results, with normalized RMSE of 27% and R2 of 0.93. This novel approach generates predictions 4700 times faster than traditional physics-based computational models, representing a paradigm shift in long-term river evolution simulations and opening new opportunities for fluvial morphodynamic modeling.

Summary

Understanding and predicting the evolution of river landscapes is critical for effective river management. Traditional physics-based morphodynamic models, while accurate, are computationally intensive and often impractical for long-term applications. This study presents a robust deep learning framework, which was designed to overcome the computational limitations by enabling rapid and reliable predictions of hydrodynamic and sediment transport behaviors.

1 Introduction

Fluvial landscapes are the nexus of the water cycle, climate, and Earth surface processes. Easy
45 access to water for domestic and agricultural needs has made river floodplains attractive places to live
throughout human history (Fang and Jawitz, 2019). Floodplains are morphodynamically active
environments continuously modified by erosional and depositional processes during floods, coupled
with lateral migration of adjacent river channels. These changes can be accompanied by significant
ecological and socio-economic impacts, including migration or destruction of sensitive habitats, loss of
50 agricultural lands, changes in navigability, destruction of infrastructure, and loss of life (Mananoma,
2009; Vercruyssen et al., 2017; Zakipour et al., 2023). Associated risks can only be offset through
effective long-term (multi-century) management planning for reach-scale geomorphic responses to
environmental perturbation (Fathi et al., 2024b). This is especially important as we plan for the impacts
of climate change on rivers, floodplains, and the communities they support.

55 Sediment transport and morphodynamic responses of rivers and floodplains have been
recorded and/or studied using remotely sensed data and projected using physics-based numerical
models (Donati et al., 2021). While significantly advancing sediment transport and morphodynamic
theory, each approach is limited. Remote sensing techniques, utilizing satellites, airplanes, and remote
vehicles (e.g., drones), represent the most practical and precise approach for morphodynamic mapping
60 (Boothroyd et al., 2021). They are limited by coarse spatial resolution in freely available imagery, high
costs for high-resolution alternatives, and short decadal record lengths (Grabowski et al., 2014). Further,
while extremely useful in understanding past landscape changes, these techniques are relatively limited
in their applicability to future change projections in assorted synthetic scenarios, e.g., climate change
studies and restoration assessment projects. Numerical models, on the other hand, can be used to
65 understand and project past and future landscape change, respectively as they include options for
synthetically modeling environments with different climatic conditions, sediment properties, and/or
channel geometries (Coulthard and Van De Wiel, 2012). The research community efforts have
developed and advanced multiple physics-based geomorphological models, such as Delft3D (Deltares,
2010), MIKE 21C (DHI, 2017), and HEC-RAS (USACE, 2021). However, these are computationally
70 expensive models, leaving users with no option but to compromise on accuracy and/or the time scales
to which they are applied (Gonzales-Inca et al., 2022).

The computer revolution brought the widespread usage of geomorphologic models to simulate
hydrodynamic and sediment transport in rivers. Models incorporate various levels of complexity,
ranging from the simplest 1D models to the most complex/advanced 3D modeling (Williams et al.,
75 2016). Choosing among these modeling dimensions requires a trade-off between accuracy,
computational resources, and applicability. The 2D approach offers a balanced combination of accuracy

and computational efficiency, enabling investigations across multiple morphological applications, e.g., river restoration (McDonald et al., 2016), the influence of dam presence (Giri et al., 2019) and dam removal (Gelfenbaum et al., 2015) on river morphology, eco-hydrology of fish habitats (Wheaton et al., 2018), vegetation dynamics (Best et al., 2018), bedform simulations (Chen et al., 2012), and bar morphology (Kasprak et al., 2019). Despite these wide-ranging applications, the 2D modeling approach is hampered by relatively long processing time and limitations on spatial and temporal scales of applicability, e.g., morphological change on relatively short between 10^0 - 10^2 km river reaches (Brasington and Richards, 2007) and timescales of just weeks or months (Williams et al., 2016). This is primarily due to: a) a need for small computational time-steps to ensure model stability (De Goede, 2020), and b) limited usage of parallel computing and/or limited capability to incorporate high computing power capabilities, e.g., graphics processing units (Karim et al., 2023).

To develop more efficient techniques for both flood hydrodynamic and geomorphological modeling, the scientific community sought solutions in Machine Learning (ML) approaches (Karim et al., 2023). Recent achievements include the usage of ML algorithms to predict flood extent maps (Avand et al., 2022; Bentivoglio et al., 2022; Ma et al., 2021; Madhuri et al., 2021; Mehedi et al., 2022; Talukdar et al., 2021). Advances in flood extent mapping spurred the development of more advanced models to predict water depth maps of flood events, e.g., artificial neural networks (ANNs) and Convolutional Neural Networks (CNNs) (Chu et al., 2020; Kabir et al., 2020). In the field of sediment transport, researchers have employed various algorithms, including random forest and support vector regression (Kwon et al., 2022), Long Short-Term Memory (LSTM) (Kaveh et al., 2021), M5 model tree (Ouellet-Proulx et al., 2016), and gated recurrent units (Huang et al., 2021), to predict suspended sediment concentrations. The focus has further extended to explore the prediction of specific sediment transport characteristics such as bed load material in channels (Hosseiny et al., 2023; Kitsikoudis et al., 2014; Sahraei et al., 2018), sediment yield during monsoon (Ghose, 2018), and sediment transport dynamics within sewer systems (Zounemat-Kermani et al., 2020). Despite these scientific efforts to advance sediment load simulations, to the best of our knowledge, no prior research has explored the usage of data-driven approaches in predicting the 2D geomorphological responses within floodplains.

To address this gap, this study aims to leverage the capabilities of Deep Learning (DL) approaches to efficiently simulate the hydrodynamic and morphodynamic behavior within floodplains. Most recently, Fathi et al. (2025) developed a Hybrid DL framework for Flood Mapping (HDL-FM) to simulate the 2D flood dynamic characteristics. This framework integrates the spatial advantages of CNN along the sequential capabilities of LSTM, to predict three essential hydrodynamic features: water depth, flow velocity, and flow direction maps. The HDL-FM framework demonstrated efficiency and robustness in capturing the spatiotemporal flood dynamic nature. Here we extend the HDL-FM framework to consider not only the hydrodynamic characteristics but also the geomorphologic behavior

mapping. The primary objective is to develop an efficient framework capable of capturing the complexity of morphodynamic processes while avoiding the computational challenges posed by traditional approaches. The resulting framework predicts the dynamics of essential hydrodynamic outputs: water depth and flow velocity, which are fundamental inputs to the morphodynamic target, represented in bed change maps. This approach presents a robust and more efficient methodology that has significant implications in several floodplain engineering applications, including 2D sediment transport simulations, assessing the impacts of climate change on the rivers' geomorphology, river rehabilitation projects, and, notably, in the realm of long-term land evolution studies.

2 Materials and Methods

2.1 Study Area and Geomorphologic Model

This study focuses on a 22 km segment of the Ninnescah River in central Kansas, a tributary of the Arkansas River (Figure 1-a). The Ninnescah River primarily has sandy banks, resulting in typically wide, shallow, and straight channels, with a bankfull width of approximately 100 m (Costigan et al., 2014). The selected river segment, with a sinuosity coefficient of two, provides an ideal case study for this research. The hourly discharge data of this segment is monitored by the United States Geological Survey (USGS) station 07145500, with a mean annual discharge of approximately 15 cms.

A 2D geomorphological simulation for the Ninnescah River segment was generated using HEC-RAS. The developed model covers a 2D grid area of 66.5 km² with 520 x 320 cells (each 20 m by 20 m). Three essential inputs are required for this type of simulation: a Digital Elevation Model (DEM) for the river including the floodplain with a high spatial resolution of 1/3 arc-second (approximately 10 meters) from USGS (2018), a flow hydrograph at the upstream boundary (USGS gage 07145500), and riverbed sediment characteristics based on the sediment samples of the riverbed collected by Costigan et al. (2014). Sediment grain sizes at D10, D50, and D90 measured 0.25 mm, 0.45 mm, and 1.1 mm, respectively. Due to the absence of bathymetry information in the DEM file, a trapezoidal cross-section profile was burned into the DEM file (Choné et al., 2018), using a channel depth of 1.1 m and a bankfull width of 95 m, informed by field measurements reported by Costigan et al. (2014). Lastly, the hydrograph component represents the driving hydrodynamic power of the flow through the system, from USGS at station 07145500.

Due to the limited availability of spatiotemporal observational data within the study reach, full calibration and independent validation of the hydraulic and sediment transport parameters were not feasible. To maintain consistency in the physics-based reference, we adopted a physically reasonable and internally coherent HEC-RAS configuration. Uniform Manning's n values of 0.035 for the main channel and 0.05 across the floodplain were applied, which fall within commonly reported ranges for

145 alluvial systems. HEC-RAS includes a wide suite of empirical sediment-transport formulations, and
for this study, the Wu equation was selected due to its demonstrated robustness in comparative
assessments against other widely used transport formulas (Wu et al., 2000). The Wu equation is well-
suited for channels with the grain size distribution of the Ninescah River, as it explicitly incorporates
the effects of nonuniform sediment mixtures and gradation (Wu and Lin, 2014). In contrast, classical
150 approaches such as Meyer-Peter-Müller or Engelund-Hansen do not incorporate bed-material
nonuniformity and may therefore yield biased transport estimates under conditions similar to those of
the study reach (Hunziker and Jaeggi, 2002). The developed model ensures that the morphodynamic
responses arise from physics-based background, thereby allowing a more direct evaluation of the DL
model's ability to replicate the nonlinear morphodynamic behavior of the physics-based solver.

155 A hydrograph with a broad range of flood events is essential to enhance the capabilities of the
DL framework in capturing hidden patterns in the mapping between inputs and outputs. Unfortunately,
generating sufficiently long training and testing datasets is hindered by the long processing time using
the physics-based model. Additionally, significant portions of the observed hydrograph are baseflow,
which corresponds to a period of relatively low flow with minimal sediment transport. To address these
160 challenges, a constructed hydrograph of 20 events was extracted from the observed hydrograph. This
event set was designed to encompass a broader range of flood magnitudes while avoiding long periods
of baseflow discharge. Repetition of similar events was intentionally avoided, as such redundancy is
unlikely to provide additional informative signals for the DL framework. This hydrograph was split into
three portions: training, validation, and testing of 11, 3, and 6 events, respectively (Figure 1-b),
165 following common data-driven modeling practice to balance model learning and independent
evaluation within computational constraints.

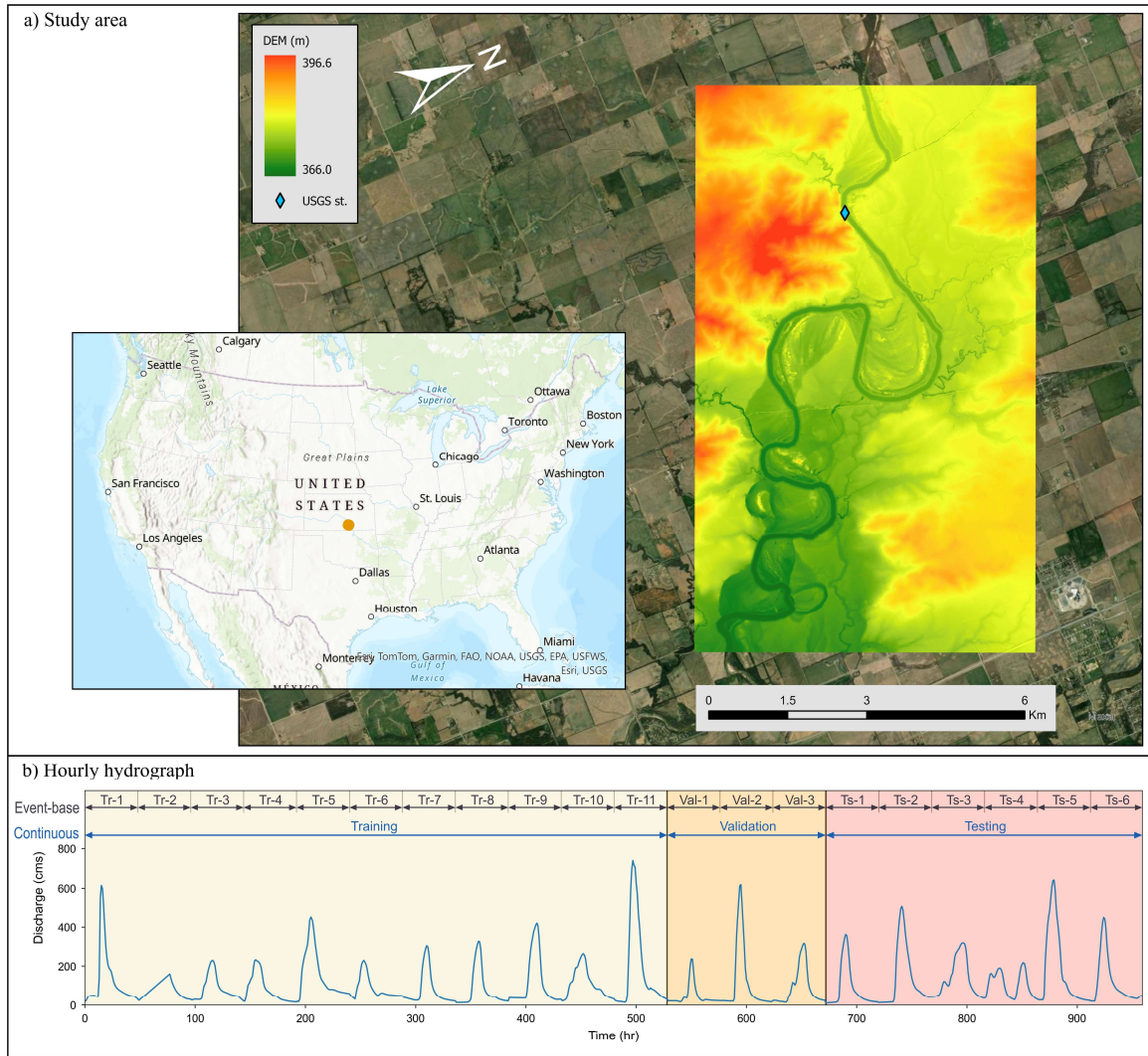


Figure 1: The case application: a) the location of the Ninesciah River segment, Kansas, USA, and b) the hourly hydrograph, divided into training, validation, and testing sets for the DL modeling.

170

The Morphological Acceleration Factor (M_f) technique is used in the HEC-RAS model to reduce the sediment transport simulation time. M_f is a scalar quantity that is used to reduce the time-step values of a hydrograph by M_f , while multiplying the calculated erosion and deposition rates by the same factor (Lesser et al., 2004). It is worth noting that there is a trade-off between utilizing a higher acceleration factor and the accuracy of the morphodynamic outputs. Morgan et al. (2020) explored this trade-off on Nooksack River in Washington through investigating a range of M_f from 5 to 50. Their results showed that M_f of 5 provided a valuable balance, reducing computational time by approximately 80% while maintaining a relatively low absolute percentage error of about 8%. In contrast, larger acceleration factors (M_f over 20) led to substantial increases in error, in some cases exceeding 30%, indicating degradation of morphodynamic fidelity. Because such nonlinearities affect both the hydrograph and the morphological responses, expert judgment remains essential for interpreting morphodynamic outputs. Based on these considerations, M_f of 5 was adopted in the present study, where

175

180

each flood event spans a full-scale of 10-days, encompassing the typical progression of flood events from initial baseflow, through the peak, and returning to baseflow, which is reduced to only 2 days using M_f of 5 (Figure 1-b).
185

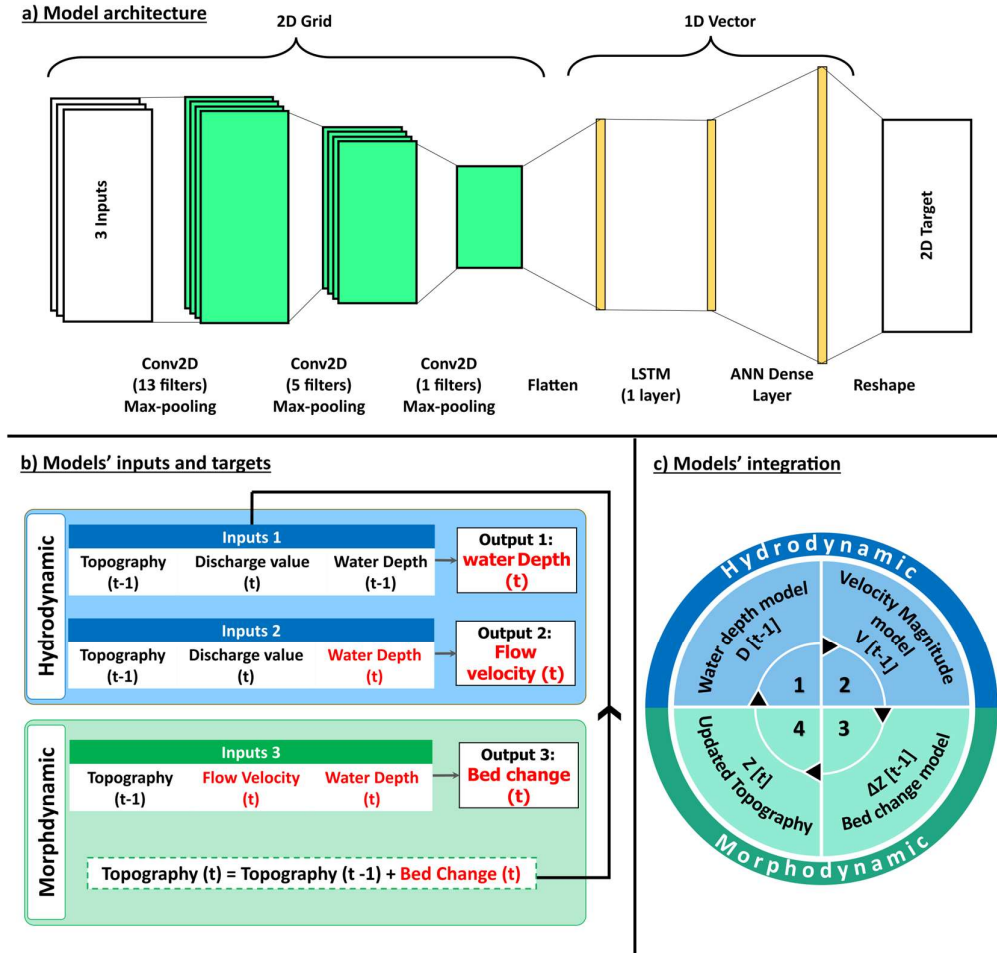
2.2 Deep Learning Model

This study aims to extend the capabilities of the Hybrid DL framework for Flood Mapping (HDL-FM), developed by Fathi et al. (2025), into geomorphology mapping (HDL-GM). This hybrid DL framework integrates the spatial strengths of Convolutional Neural Networks (CNN) coupled with
190 the temporal prowess of Long Short-Term Memory (LSTM). CNNs perform automated feature engineering through learnable filters, enabling the detection and extraction of spatial features from the inputs. Multiple layers of CNNs build a hierarchy of increasingly complex features, ultimately enabling the recognition of objects within the 2D grids (Bhatt et al., 2021). LSTM is a powerful type of recurrent neural network designed to handle sequential data (Fathi et al., 2025; Kratzert et al., 2018; Yu et al.,
195 2019). LSTMs incorporate memory cells with input, output, and forget gates, allowing the network to selectively remember or forget information over long sequences.

HDL-FM is an integrated DL model combining CNN and LSTM (Figure 2-a), originally developed to predict the hydrodynamic properties of flood events in 2D grids. This study incorporates this approach into geomorphologic modeling by using it to capture sediment transport. This framework
200 encompasses three models, all of which have the same architecture (Figure 2-a), but with different targets: water depth, flow velocity, and bed change. This framework utilizes a uniform 2D shape of 520 x 320 grid (each 20 m by 20 m) for both inputs and targets, ensuring compatibility with the HEC-RAS model simulation. Each model commences with an encoder block comprised of three CNN layers, each followed by a rectified linear unit (ReLU) activation function. A 2x2 max-pooling operation was
205 applied to each layer, balancing the preservation of high-resolution morphology features in narrow river segments with improved computational efficiency through a reduction of grid size by half. It should be noted that large pool sizes tend to lose important details in the segment meanders, affecting morphodynamic predictions. In the encoder phase, a flattening process is applied, generating a single vector suitable for processing by a single LSTM layer. The enhancement in prediction accuracy through
210 utilizing additional LSTM layers was minimal. An ANN dense layer is introduced as a decoder stage where the LSTM outputs convert back into a long vector possessing the same number of elements as the physics-based grid, to reconstruct the original grid dimension.

This study explores the applicability of a hybrid DL model to predict the hydrodynamic and morphodynamic behavior of flood events at 30-min intervals according to three models: water depth,
215 flow velocity, and bed change. Each model utilizes a distinct set of inputs as described in Figure 2-b. In contrast to the original framework, the geomorphological version, HDL-GM, incorporates a

temporally varying topographic input (Z). To standardize the topography input, a simple normalization process is applied through subtracting the average elevation value, calculated at the beginning of the simulation, from the entire topography grid. Additionally, other dynamic inputs are introduced to the framework, including water depth (D), flow velocity (V), and discharge value (Q) at the upstream boundary condition. The upstream discharge series is transformed into a grid initialized with zeros, where the Q value is subsequently assigned to a 7x7 cell block at the upstream point of the reach. To maximize the efficiency of the HDL framework as a physics-based emulator, the model was designed to learn the final morphodynamic response produced by HEC-RAS rather than to replicate intermediate sediment-transport processes. Accordingly, the HDL architecture was trained to predict bed-level change directly, using hydrodynamic fields (water depth and flow velocity) together with the upstream hydrograph as inputs. This reduced-input configuration was intentionally adopted to evaluate the model's capacity to infer the morphodynamic patterns from the essential driving variables, while avoiding additional complexity associated with explicitly modeling suspended sediment, bedload transport rates, or sediment-property fields. The proposed three models employ lagged input variables from the previous time-step to predict the targets at the subsequent time-step targets, such as the topography and water depth grids (Figure 2-b). Conversely, other inputs, encompassing the flow velocity and upstream discharge, are utilized from the current time-step.



235 Figure 2: An overview of the HDL-FM model, where a) model architecture, b) model inputs and targets, and c) sequential model integration for the testing procedure.

The training process for the proposed framework employs the smooth L_1 loss function for enhanced convergence stability and robustness to outliers (Girshick, 2015). Optimization is performed using the Adam optimizer (Kingma and Ba, 2015), with the learning rate dynamically adjusted throughout the training process using the ReduceLROnPlateau technique to ensure efficient and rapid convergence (Al-Kababji et al., 2022; PyTorch, 2024).

2.3 Model Evaluation and Performance Criteria

Testing Mechanism:

245 The dynamic nature of geomorphic simulations, which continuously evolves over time, depends on lagged inputs from previous time-steps to predict the system's behavior at the following time-steps. Evaluating the capabilities of these models to operate independently, without prior reference inputs, is essential. To address this, a four-step loop was developed to assess the accuracy of the proposed framework in real-world applications (Figure 2-c). At a typical time-step, the framework starts

250 with predicting the water depth, which serves as an essential input for the subsequent step of predicting
the flow velocity. In the third step, the bed change of the topography is predicted based on outputs from
the first two steps. Finally, the loop concludes by using the bed change output to update the topography
grid, which serves as the primary input of the loop at the next time-step. This loop is applied iteratively
to the testing dataset, allowing the framework to predict its own future inputs without relying on any
255 reference inputs. This testing technique is introduced to evaluate the framework's robustness for long-
term simulations, to ensure that it can operate without error accumulation issues.

Performance Criteria:

To evaluate the accuracy of the proposed model in predicting the hydrodynamic and bed
change variables, Root Mean Square Error (RMSE) is used to quantify the average magnitude of errors
260 between HDL-GM predictions and reference results obtained from the HEC-RAS model (Eq. 1)
(Stigler, 1990), and assesses the accuracy at a single time-step or is averaged across the testing period.
However, using the total number of cells (including the cells without any morphodynamic behavior) in
estimating the average could lead to misleading accuracy values. To address this challenge, the cells
considered in the RMSE are restricted to the active cells, which represent the locations within the
265 predicted or reference grids where water depth or bed change exceeds 0.05 m or 0.02 m, respectively.
However, because the bed change values increase progressively over time, RMSE alone can be
misleading to track the model performance over time. To address this, Normalized Root Mean Square
Error (NRMSE) is introduced to normalize RMSE into a percentage relative to the root mean square of
the target values (Eq. 2), thereby facilitating a more meaningful and consistent comparison of prediction
270 errors across different time steps (Mentaschi et al., 2013). Additionally, the coefficient of determination
(R^2) is employed as a complementary metric (Eq. 3) (Veall and Zimmermann, 1996). R^2 evaluates how
effectively the model captures the underlying distribution of the data, in this case regarding erosional
and depositional activities across the grid domain.

$$\text{RMSE} = \sqrt{\frac{1}{N} \sum_{i=1}^N (R_i - S_i)^2} \quad \text{Eq. 1}$$

$$\text{NRMSE} = \frac{\text{RMSE}}{\sqrt{\frac{1}{N} \sum_{i=1}^N (R_i)^2}} \quad \text{Eq. 2}$$

$$R^2 = 1 - \frac{\sum_{i=1}^N (R_i - S_i)^2}{\sum_{i=1}^N (R_i - \bar{R})^2} \quad \text{Eq. 3}$$

where R_i, S_i are the physics-based reference values obtained from HEC-RAS and the corresponding
275 simulated values predicted by the HDL-GM framework, respectively, and \bar{R} is the average value of
reference grids. N is the number of active cells within the predicted or reference domains. These

performance criteria are applicable to both the hydrodynamic components (water depth and flow velocity) and the morphodynamic component (bed elevation change).

280 Although NRMSE and R^2 provide useful global measures of model performance, geomorphic responses are spatially heterogeneous and cannot be fully described by a single performance value. To better capture spatial error patterns, cell-scale absolute and relative error maps were developed, comparing the physics-based HEC-RAS reference results with the HDL-GM predictions. Absolute error represents the absolute difference between the reference and predicted values at cell-scale, with a perfect value of zero and no upper bound. Relative error expresses this absolute error normalized by the
285 reference value at each cell, enabling comparison across regions with differing response magnitudes. While relative error also attains an optimal value of zero, it may exceed 100% in areas where predictions are large relative to the reference bed change values or the reference bed change values are marginal. Performance criteria along spatial error metrics provide a more complete assessment of both the magnitude and significance of prediction errors across the domain.

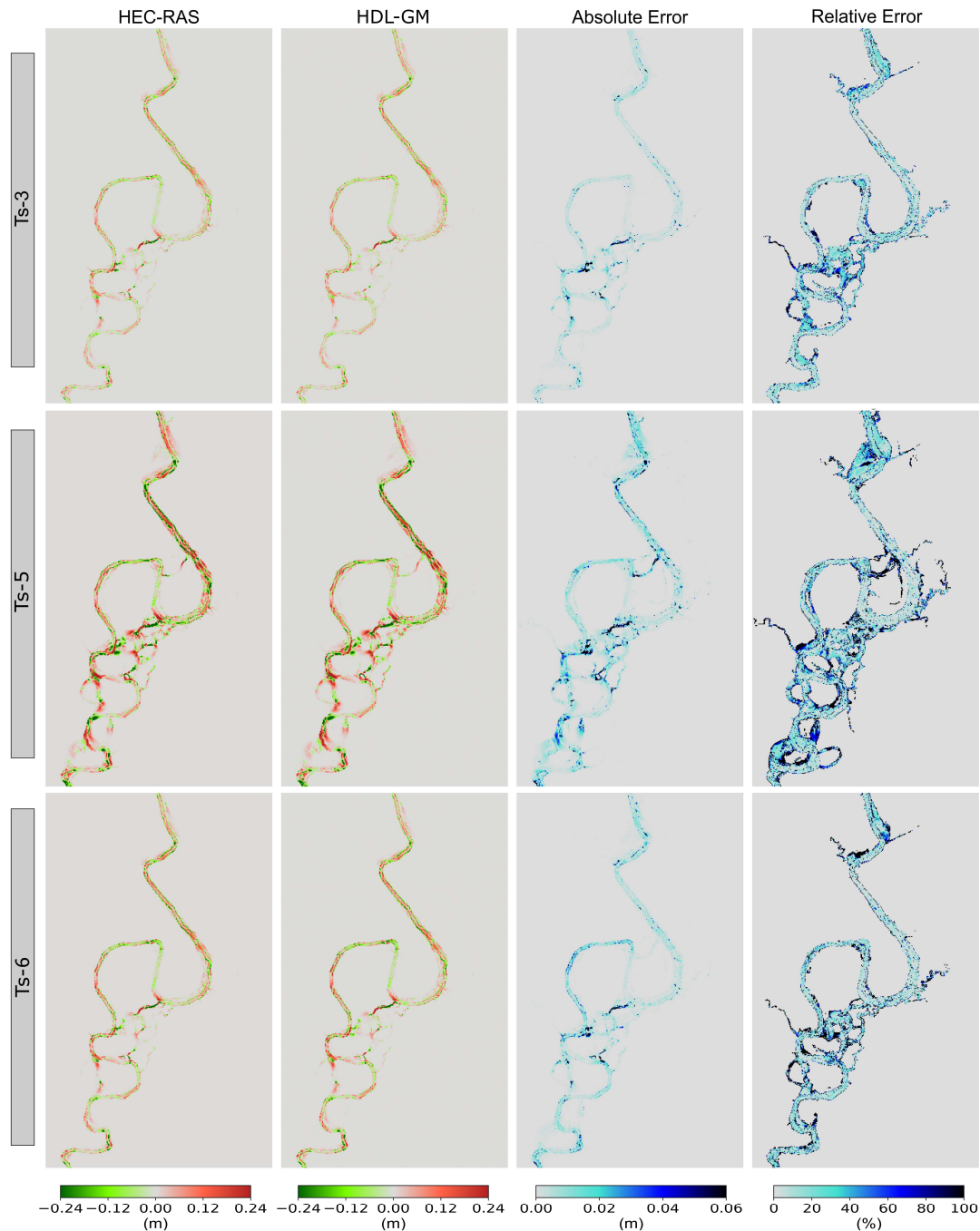
290 **3 Results and Discussion**

Two distinct versions of the HDL-GM framework were tested. These versions are based on the nature of the training dataset: Event-Based (EB) and Continuous-Based (CB) datasets (Figure 1-b). The EB dataset aggregates discrete events that are simulated independently using the physics-based model, each initialized from the same topographic state. This formulation enhances computational
295 efficiency in generating the training dataset by allowing parallel simulations. Conversely, the CB dataset is derived from a single temporally continuous simulation that spans a sequence of events, which demands significantly longer processing time due to its continuous simulation to resolve the full temporal evolution of the system. To assess the performance and trade-offs of these models, three experimental scenarios were implemented: 1) the EB-trained framework tested on the EB dataset, 2)
300 the EB-trained framework tested on the CB dataset, and 3) the CB-trained framework tested on the CB dataset. These scenarios were designed to investigate the tradeoff between the computational efficiency of dataset generation and the accuracy of the framework in both EB and CB applications.

3.1 EB-Trained HDL-GM Framework for Geomorphic Simulation

For the EB-trained HDL-GM framework, both water depth and flow velocity models exhibit
305 strong agreement with reference data from HEC-RAS, where the average RMSE values, across the entire testing dataset, are 0.19 m and 0.04 m/s, respectively. These low RMSE values not only underscore the robust hydrodynamic capabilities of this approach but are also essential for accurate geomorphic predictions.

The HDL-GM framework integrated the outputs of both hydrodynamic models, water depth
310 and flow velocity, as inputs for the bed change model. Figure 3 illustrates the bed change results at the
end of three testing events. The bed change model within the proposed framework exhibited robust
capabilities in accurately predicting the spatial patterning of erosional and depositional processes across
the grid domain, as compared to HEC-RAS results. This is evidenced by the low RMSE values, across
the testing six events, ranging from 0.02 to 0.03 m, with a mean of 0.026 m. It should be noted that
315 most of the high relative errors were concentrated in shallow wetland areas, where the morphodynamic
activities are primarily forced by shallow overbank flow. This may be attributed to the minimal
magnitude of bed changes in these regions, with high uncertainties. Consequently, when the error is
normalized by these small bed changes, it results in high relative errors.



320 Figure 3: Comparison of bed change predictions of EB-testing dataset by HEC-RAS and EB-trained
 HDL-GM framework for the three testing events, illustrating the spatial distribution of absolute error
 and relative error between both models, where Ts denotes a specific flood event in the testing dataset.

325 The EB-trained framework exhibited robust performance in accurately predicting the bed
 change of the EB-testing dataset. However, it is crucial to assess its performance on the CB-testing
 dataset, which is characterized by cumulative geomorphic behavior across multiple events. Figure 4
 presents the absolute and relative error results at the end of multiple testing events within the CB dataset.
 The EB-trained framework maintained acceptable performance during the first couple of events; but

after three events, a noticeable accumulation of error values emerged. By the end of the CB simulation, the relative error exceeded 100% at numerous locations both within the stream channel and shallow areas. While the EB-trained HDL-GM framework, based on an efficient EB-training dataset, demonstrated strong predictive capabilities for the EB-testing dataset, its performance on the CB-testing dataset revealed significant and unacceptable error accumulation. This behavior could potentially be attributed to the nonlinearity of sediment transport over multiple flood events, which may not be fully represented in the EB dataset. These findings underscore its limitations in capturing the complexities of continuous morphodynamic processes.

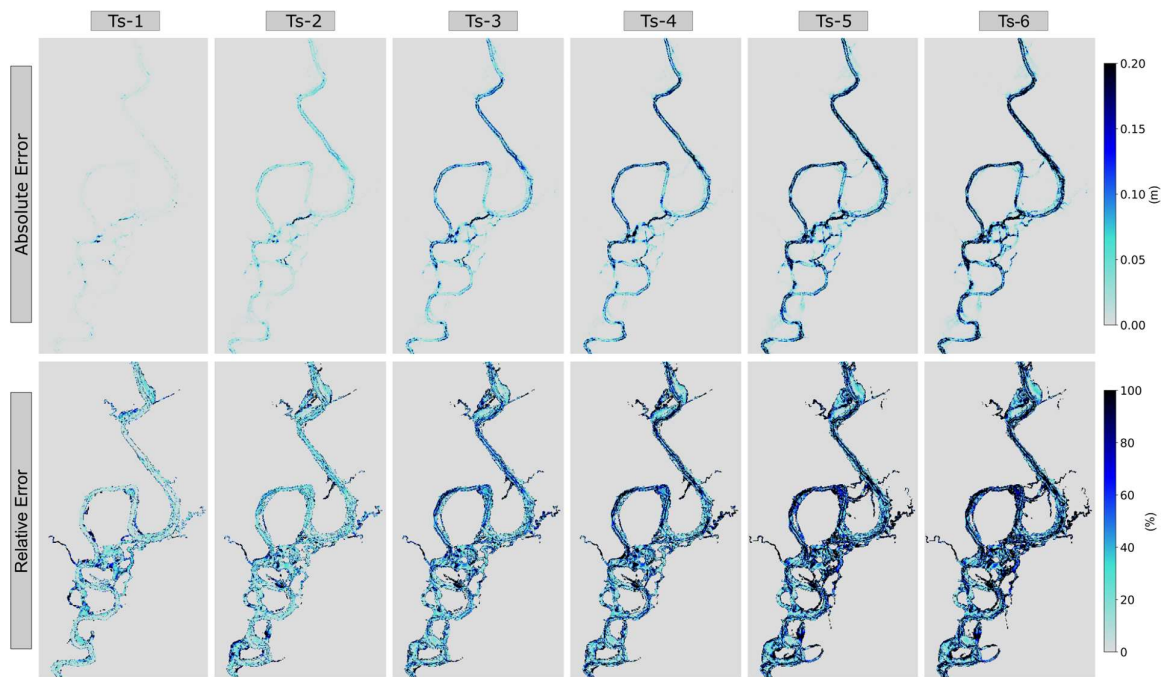


Figure 4: Absolute error and relative error of using EB-trained HDL-GM framework to predict bed change for CB-testing dataset.

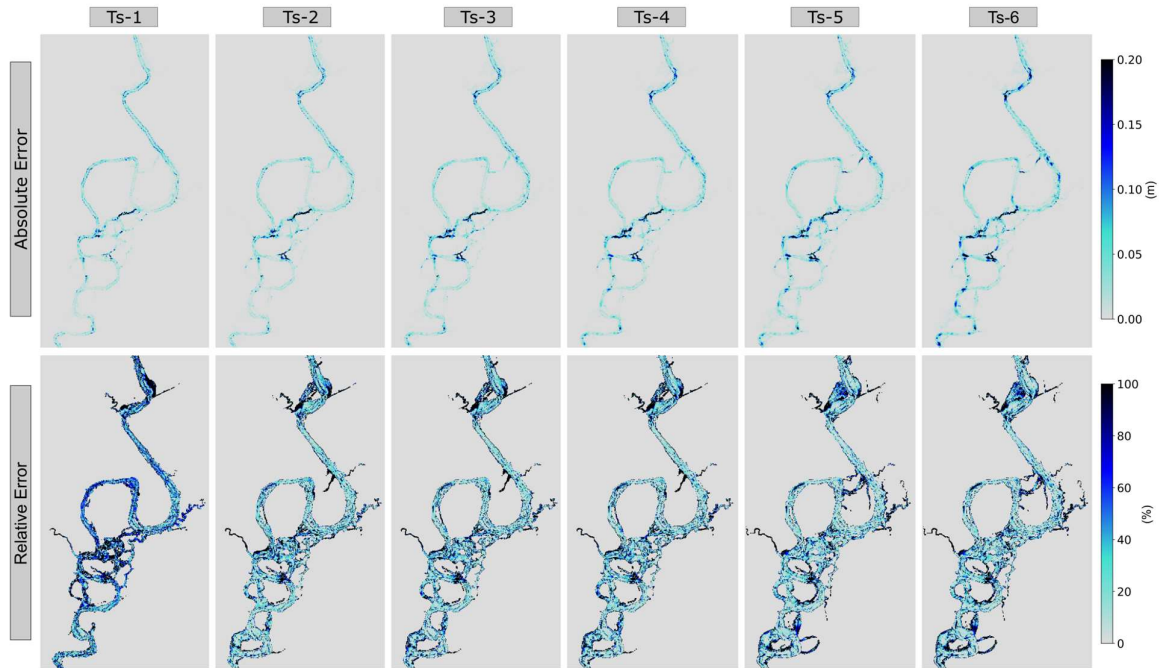
340

3.2 CB-Trained HDL-GM Framework for Geomorphic Simulation

The CB-trained framework exhibited strong performance in predicting hydrodynamic features, with mean RMSE values of 0.15 m for water depth and 0.04 m/s for flow velocity variables, across the entire testing dataset. These hydrodynamic outputs were subsequently integrated into the bed change model. Figure 5 presents the absolute and relative error results at the end of multiple testing events within the CB dataset. Initially, the CB-trained framework maintained relatively high relative errors at the end of the first testing event, primarily because the reference bed-change magnitudes during this first event are small; as a result, even minor absolute deviations from the HDL-GM predictions translate into large relative errors. After this first event, it exhibited rapid recovery, yielding substantially reduced relative errors from the second testing event. This robust performance continued throughout the CB testing dataset, with no accumulation of relative errors. This is further evidenced by

350

an RMSE value of 0.07 m at the end of the sixth event. These findings highlight the capabilities of the CB-trained framework to predict morphodynamic behavior across a testing dataset encompassing a series of continuous events. Nevertheless, while the HDL-GM framework remains stable, the maximum forward prediction horizon over which robust morphodynamic predictions can be maintained requires further investigation, beyond the scope of this study, and is expected to depend on numerous factors such as hydrologic forcing, geomorphic nonlinearity, and the inductive biases of the DL architecture itself.



360 Figure 5: Absolute error and relative error of testing CB-trained HDL-GM framework to predict bed change for CB-testing dataset.

3.3 Statistical Comparison of EB and CB-Trained Frameworks

To evaluate the performance of the EB and CB-trained frameworks, a comprehensive statistical comparison was conducted across three previously defined scenarios. The assessment utilized four performance criteria: RMSE, NRMSE, 95% error, and R^2 , as represented in Figure 6. The 95% error is defined as the threshold below which 95% of the cell-scale absolute errors across all active cells fall, corresponding to the 95th percentile of the absolute error distribution. Consequently, it offers additional insight beyond mean-based statistics by quantifying the magnitude of errors affecting the vast majority of active cells, defined here as cells exhibiting bed changes greater than 0.02 m. For the EB-testing dataset, results are presented separately at the end of each event. In contrast, the results for the CB-testing dataset are cumulative, extending from the start of the simulation to the end of a given event. The key findings from this comparative analysis are outlined as follows.

- 375 Scenario 1: the EB-trained framework demonstrated robust performance when applied to the EB-testing dataset. Performance metrics indicated consistent predictive accuracy with mean NRMSE and R^2 of 22% and 0.94, respectively; this suggests that the framework effectively captures event-based dynamics.
- 380 Scenario 2: when applied to the CB-testing dataset, the EB-trained framework initially showed acceptable performance for the first two events. However, subsequent events revealed a significant degradation in predictive accuracy due to error accumulation. The NRMSE escalated from an initial value of 21% to 113% by the end of the sixth event, which yielded a negative R^2 value. Over time, the error becomes untenable.
- 385 Scenario 3: the CB-trained framework exhibited superior adaptability and stability when applied to the CB-testing dataset. The framework's performance improved markedly after the first one or two events. The NRMSE decreased from an initial value of 66% to less than 27%, at the end of the testing dataset. It is worth noting that the RMSE values demonstrated remarkable stability, within a narrow band of 0.06 to 0.07 m, throughout the simulation.

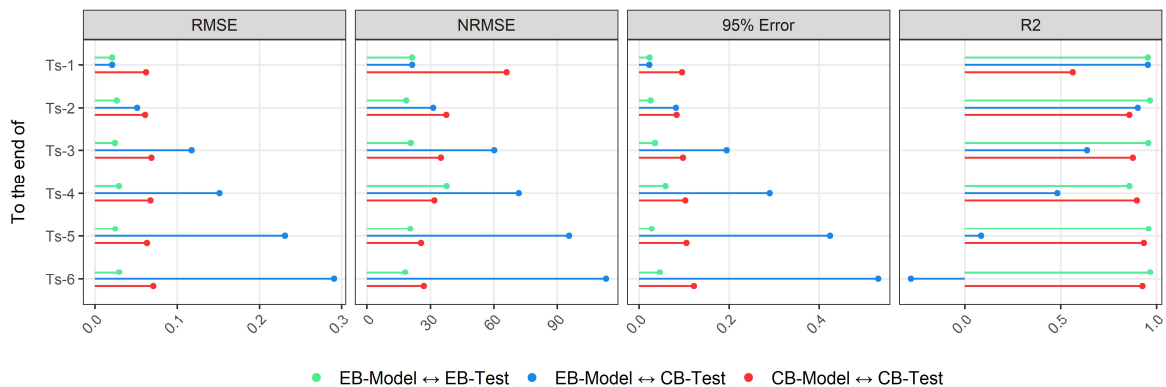


Figure 6: Evaluation statistics of the EB and CB-trained frameworks on the EB and CB-testing datasets.

390

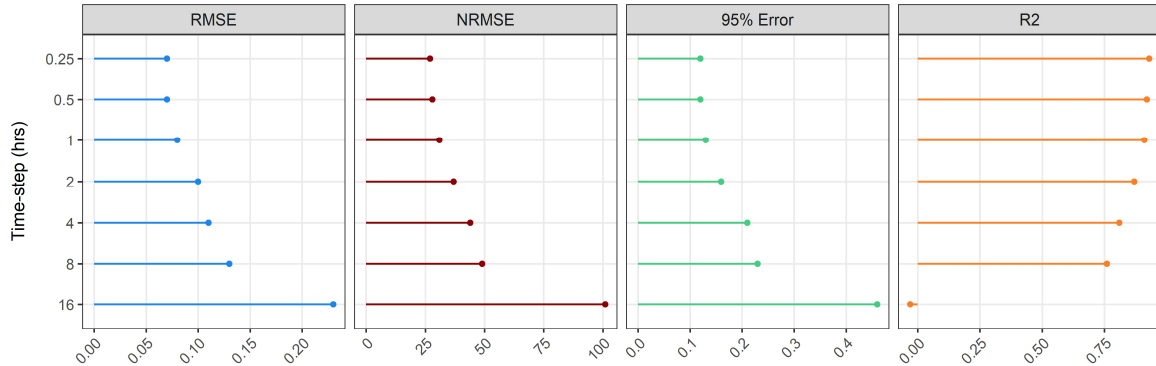
3.4 The Influence of Temporal Resolution on CB-Trained HDL-GM Accuracy

The temporal resolution of a model framework profoundly influences training efficiency, prediction accuracy, and the model's capacity to fulfill specific application requirements, thereby shaping its overall effectiveness and utility. The CB-trained HDL-GM framework was assessed using datasets with varying time-steps, ranging from 0.25-hr to 16-hr (Figure 7). The framework trained on datasets with time-steps of 0.25, 0.5, and 1-hr time-steps demonstrated relatively consistent performance, maintaining a consistent NRMSE of less than 30%. However, coarser time-steps, of 2, 4, and 8-hr, led to a decline in predictive capabilities, as evidenced by a reduction in R^2 values from 0.90 to 0.76. This performance deteriorated significantly for the 16-hr time-step configuration, exhibiting an NRMSE exceeding 100% and a negative R^2 value. This analysis suggests that beyond the 8-hr threshold,

395

400

coarser resolution reduces the model’s ability to accurately capture the hydrodynamic peaks of flood events, thereby impacting the accuracy of morphodynamic predictions. These findings suggest that there is a potential relationship between the hydrodynamic scale of the system and the optimal temporal resolution of the modeling framework, warranting further research in this area as a future endeavor.



405

Figure 7: Evaluation statistics of the CB-Model for various temporal resolutions at the end of the simulation.

3.5 Comparison of Prediction Runtimes Between Physics-Based and HDL-GM Models

410

The prediction runtime and computational demands have been critical considerations in the morphodynamic modeling approach. This section highlights the substantial efficiency gains achieved by the proposed HDL-GM framework relative to the HEC-RAS simulations. Notably, HEC-RAS requires a 3-second computational time step to maintain numerical stability in both hydrodynamic and sediment-transport solvers. This constraint is a major source of the long processing times associated with physics-based models. In contrast, the HDL-GM framework is not limited by such stability limitations and can therefore operate at much coarser time steps, allowing evaluations at coarser resolutions, enabling the substantial computational speedup demonstrated by the DL-based approach.

415

420

A comprehensive processing time assessment was conducted by comparing the HEC-RAS model, executed on an Intel-based laptop, with the HDL-GM framework, trained on both the same laptop system and Augie, Villanova Engineering’s High-Performance Computing Cluster (HPC), as presented in Table 1. Building upon the previous section's findings, the HDL-GM framework was trained using a dataset with a 1-hr time-step, due to its proven efficiency and accuracy. The results of the training stage and the predictions of a 528-hr duration are presented in Table 1. The key findings from this comparative analysis are outlined as follows.

425

- The processing time of HEC-RAS is considerably long, requiring over 13 days to complete a 528-hr simulation.

430

- The HDL-GM framework’s training stage exhibited significant efficiency, particularly in the HPC environment, where parallel training of the three models was completed in about 2.25-hr. In contrast, training on a standard laptop, which necessitated a series approach, required about 11-hr.
- The prediction runtime for the trained framework demonstrated remarkable efficiency. By executing the loop between the water depth, flow velocity, and bed change models, the HDL-GM framework operates at a rate that is 4700 times faster than the physics-based model, regardless of whether the HPC or the laptop was utilized.

435

Table 1: Computational time of HEC-RAS vs HDL-GM at two distinct computational systems. All time values are in minutes.

Model	Machine	Target	Training		Predictions
			Processing time	Total time	Total time
HEC-RAS	Laptop				18900
HDL-GM	Laptop	Water depth	213	671 (series)	4
		Velocity magnitude	142		
		Bed change	316		
	HPC	Water depth	136	136 (parallel)	4
		Velocity magnitude	73		
		Bed change	112		

Laptop: Intel® Core™ i9-13900H + 32 GB LPDDR5 RAM

HPC: 64 AMD EPYC Series CPU Cores

4 Conclusions

440

Computational morphodynamic models are important for simulating the erosional and depositional processes associated with moving rivers and changing landscapes. However, the computational demands of these models result in prolonged processing times, thereby limiting their utility in long-term simulations. To address this shortcoming, many researchers have explored data-driven algorithms in predicting sediment transport rates with numerous applications. However, to our knowledge, no prior research has focused on leveraging the capabilities of DL in predicting 2D geomorphic evolution of river floodplains.

445

This study introduces a novel DL framework designed to address the computational challenges of physics-based models, enabling robust, rapid, and reliable generation of 2D morphodynamic maps. Given the lack of observational data for the Ninescah River, this study does not aim to optimize agreement with field measurements; instead, it evaluates the capacity of the DL model to reproduce the spatiotemporal dynamics generated by a physics-based numerical solver. For

450 this purpose, the HEC-RAS model was used as a synthetic reference generator, providing internally consistent hydrodynamic and morphodynamic responses. This learning approach, widely used in surrogate modeling and increasingly adopted in Earth-surface research where observational datasets are sparse, leverages a synthetic, noise-free, and complete dataset to enable robust DL training while avoiding the practical constraints of field data collection (De Melo et al., 2022).

455 This novel framework represents a major step in geomorphologic prediction, through a full-system simulator of the complex interaction of hydrodynamics of flood events and morphodynamic processes in fluvial areas, through integrating the spatial advantages of CNN with temporal sequences of the LSTM algorithm. The effectiveness of this spatiotemporal framework represents a powerful extension of most DL implementations, which are either sequentially dynamic point-scale applications
460 or static spatially distributed simulations (Bennett et al., 2024). The testing technique was developed to assess the framework's capabilities in real-world scenarios, where the three models, water depth, flow velocity, and bed change, operate iteratively in a loop.

Additionally, a comprehensive analysis was conducted to evaluate the trade-off between the efficiency of generating training datasets and their corresponding predictive accuracy. Two
465 methodologies were compared: EB, representing an efficient dataset generation approach, and CB, a computationally intensive alternative, through three experimental scenarios: 1) the EB-trained framework tested on the EB dataset, 2) the EB-trained framework tested on the CB dataset, and 3) the CB-trained framework tested on the CB dataset. Some key findings from this study include the following.

- 470 • Both EB and CB-trained frameworks exhibited strong performance in predicting both hydrodynamic features: water depth and flow velocity, whereas the CB-trained framework had slightly superior performance.
- Despite the robust capabilities of the EB-trained framework in predicting the spatiotemporal bed change activities of the EB-testing dataset, its performance on the CB-testing dataset
475 exhibited significant limitations, characterized by a pronounced accumulation of errors. As a result, the model performance significantly decreased after a few flood events.
- The CB-trained framework demonstrated superior performance and strong stability when applied to the CB-testing dataset, with a very narrow range of RMSE of 0.06 to 0.07 m, throughout the testing evaluation, showing consistent performance over time.
- 480 • Consistent accuracy in simulating morphodynamics was achieved across multiple temporal resolutions: 0.25, 0.5, and 1-hr, demonstrating the framework's versatility in meeting diverse

application requirements. However, as the timesteps became coarser, the model performance became worse.

- The HDL-GM framework achieved a remarkable speedup of over 4700 compared to the HEC-RAS model. This significant efficiency gain is secured through the transition from a second-based time-step of physics-based models to an hourly time-step, by leveraging the capabilities of the DL approach.

Ultimately, the proposed framework demonstrates significant potential in enhancing morphodynamic modeling in fluvial rivers and floodplains, particularly from the long-term perspective, climate change assessments, river rehabilitation projects, and other investigations requiring long-term simulations. Despite these promising capabilities, its primary limitation lies in its inability to effectively simulate unseen topographical conditions. In addition, the current application is limited to a single-reach with one upstream boundary condition; future work should therefore evaluate the framework's performance in larger and more complex river–floodplain networks with multiple boundary conditions. The current implementation is also tailored to a particular set of hydrodynamic and sediment transport properties, especially Manning n, grain-size distributions, and cohesive properties, which may limit generalizability. Addressing these constraints will require integrating essential hydrodynamic and sediment transport physics into the DL framework (Karniadakis et al., 2021; Mohamad et al., 2021).

500 **Acknowledgments**

This work was supported by NSF under Award No: 1844180. For this study, the authors utilized the Augie High-Performance Computing cluster, at Villanova University. The authors would also like to acknowledge and thank Dr. Aaron Wemhoff for his assistance and for sharing his insight with Augie. This work was also partially supported by the Villanova Center for Resilient Water Systems (VCRWS). Nataraj and Liu were partially supported by a grant from Office of Naval Research (N00014-22-1-2480, PM: Lynn Petersen).

CRedit authorship contribution statement

Mohamed M. Fathi: Conceptualization, Methodology, Software, Validation, Data Curation, Writing - Original Draft, Visualization. Zihan Liu: Methodology, Funding acquisition, Validation, Writing - Review & Editing. Anjali M. Fernandes: Conceptualization, Funding acquisition, Writing - Review & Editing. Michael T. Hren: Conceptualization, Funding acquisition, Writing - Review & Editing. Dennis O. Terry: Conceptualization, Funding acquisition, Writing - Review & Editing. C. Nataraj: Conceptualization, Methodology, Funding acquisition, Validation, Writing - Review &

515 Editing. Virginia Smith: Conceptualization, Methodology, Supervision, Funding acquisition,
Validation, Writing - Review & Editing.

Open Research Section

520 The codes and training dataset that were used to build the HDL-GM model to simulate the
flood and geomorphic dynamic maps using Python language, based on Pytorch library, can be found on
GitHub: <https://github.com/m-fathi-said/Flood-Modeling-HDL-FM.git>. This repository was created by
Mohamed M. Fathi (msaid@fgcu.edu / m.fathi.said0@gmail.com) in 2024 under the MIT License.

References

- 525 Al-Kababji, A., Bensaali, F., Dakua, S.P., 2022. Scheduling techniques for liver segmentation: Reducelronplateau vs onecyclelr, in: International Conference on Intelligent Systems and Pattern Recognition. Springer, pp. 204–212.
- Avand, M., Kuriqi, A., Khazaei, M., Ghorbanzadeh, O., 2022. DEM resolution effects on machine learning performance for flood probability mapping. *J. Hydro-Environment Res.* 40, 1–16.
- 530 Bennett, A., Tran, H., De la Fuente, L., Triplett, A., Ma, Y., Melchior, P., Maxwell, R.M., Condon, L.E., 2024. Spatio-temporal machine learning for regional to continental scale terrestrial hydrology. *J. Adv. Model. Earth Syst.* 16, e2023MS004095.
- Bentivoglio, R., Isufi, E., Jonkman, S.N., Taormina, R., 2022. Deep learning methods for flood mapping: a review of existing applications and future research directions. *Hydrol. Earth Syst. Sci.* 26, 4345–4378.
- 535 Best, Ü.S.N., Van der Wegen, M., Dijkstra, J., Willemsen, P., Borsje, B.W., Roelvink, D.J.A., 2018. Do salt marshes survive sea level rise? Modelling wave action, morphodynamics and vegetation dynamics. *Environ. Model. Softw.* 109, 152–166.
- Bhatt, D., Patel, C., Talsania, H., Patel, J., Vaghela, R., Pandya, S., Modi, K., Ghayvat, H., 2021. CNN variants for computer vision: History, architecture, application, challenges and future scope. *Electronics* 10, 2470.
- 540 Boothroyd, R.J., Williams, R.D., Hoey, T.B., Barrett, B., Prasojo, O.A., 2021. Applications of Google Earth Engine in fluvial geomorphology for detecting river channel change. *Wiley Interdiscip. Rev. Water*. <https://doi.org/10.1002/wat2.1496>
- Brasington, J., Richards, K., 2007. Reduced-complexity, physically-based geomorphological modelling for catchment and river management. *Geomorphology*.
- 545 Chen, J., Wang, Z., Li, M., Wei, T., Chen, Z., 2012. Bedform characteristics during falling flood stage and morphodynamic interpretation of the middle–lower Changjiang (Yangtze) River channel, China. *Geomorphology* 147, 18–26.
- Choné, G., Biron, P.M., Buffin-Bélanger, T., 2018. Flood hazard mapping techniques with LiDAR in the absence of river bathymetry data, in: *E3S Web of Conferences*. EDP Sciences, p. 6005.
- 550 Chu, H., Wu, W., Wang, Q.J., Nathan, R., Wei, J., 2020. An ANN-based emulation modelling framework for flood inundation modelling: Application, challenges and future directions. *Environ. Model. Softw.* 124, 104587.
- Costigan, K.H., Daniels, M.D., Perkin, J.S., Gido, K.B., 2014. Longitudinal variability in hydraulic geometry and substrate characteristics of a Great Plains sand-bed river. *Geomorphology* 210, 48–58.
- 555 Coulthard, T.J., Van De Wiel, M.J., 2012. Modelling river history and evolution. *Philos. Trans. R. Soc. A Math. Phys. Eng. Sci.* 370, 2123–2142.
- De Goede, E.D., 2020. Historical overview of 2D and 3D hydrodynamic modelling of shallow water flows in the Netherlands. *Ocean Dyn.* 70, 521–539.
- 560 De Melo, C.M., Torralba, A., Guibas, L., DiCarlo, J., Chellappa, R., Hodgins, J., 2022. Next-generation deep learning based on simulators and synthetic data. *Trends Cogn. Sci.* 26, 174–187.

- Deltares, 2010. Delft3D-FLOW. Simulation of Multi-Dimensional Hydrodynamic Flow and Transport Phenomena, Including Sediments: User Manual. Version 3.04, Deltares, Delft, The Netherlands.
- 565 DHI, 2017. MIKE 21C, curvilinear model for river morphology, user guide. MIKE Powered by DHI.
- Donati, D., Stead, D., Brideau, M.-A., Ghirotti, M., 2021. Using pre-failure and post-failure remote sensing data to constrain the three-dimensional numerical model of a large rock slope failure. *Landslides* 18, 827–847.
- 570 Fang, Y., Jawitz, J.W., 2019. The evolution of human population distance to water in the USA from 1790 to 2010. *Nat. Commun.* 10, 1–8.
- Fathi, M.M., Al Mehedi, M.A., Smith, V., Fernandes, A.M., Hren, M.T., Terry Jr, D.O., 2025. Evaluation of LSTM vs. conceptual models for hourly rainfall runoff simulations with varied training period lengths. *Sci. Rep.* 15, 15820.
- 575 Fathi, M.M., Liu, Z., Fernandes, A.M., Hren, M.T., Terry, D.O., Nataraj, C., Smith, V., 2024a. Spatiotemporal Flood Depth and Velocity Dynamics Using a Convolutional Neural Network Within a Sequential Deep-Learning Framework. *Environ. Model. Softw.* 106307.
- Fathi, M.M., Smith, V., Awadallah, A.G., Fernandes, A.M., Hren, M.T., Terry, D.O., 2024b. Constructing Long-Term Hydrographs for River Climate-Resilience: A Novel Approach for Studying Centennial to Millennial River Behavior. *Water Resour. Res.* 60, e2024WR037666.
- 580 Gelfenbaum, G., Stevens, A.W., Miller, I., Warrick, J.A., Ogston, A.S., Eidam, E., 2015. Large-scale dam removal on the Elwha River, Washington, USA: Coastal geomorphic change. *Geomorphology* 246, 649–668.
- Ghose, D.K., 2018. Sediment yield prediction using neural networks at a watershed in south east India. *ISH J. Hydraul. Eng.* 24, 230–238.
- 585 Giri, S., Omer, A., Shrestha, B., Kayastha, N., Froehlich, D.C., 2019. Significance of geomorphological processes for safety and sustainability of water infrastructures, in: 14th International Symposium on River Sedimentation.
- Girshick, R., 2015. Fast r-cnn, in: *Proceedings of the IEEE International Conference on Computer Vision*. pp. 1440–1448.
- 590 Gonzales-Inca, C., Calle, M., Croghan, D., Torabi Haghighi, A., Marttila, H., Silander, J., Alho, P., 2022. Geospatial artificial intelligence (GeoAI) in the integrated hydrological and fluvial systems modeling: Review of current applications and trends. *Water* 14, 2211.
- Grabowski, R.C., Surian, N., Gurnell, A.M., 2014. Characterizing geomorphological change to support sustainable river restoration and management. *Wiley Interdiscip. Rev. Water* 1, 483–512.
- 595 Hosseiny, H., Masteller, C.C., Dale, J.E., Phillips, C.B., 2023. Development of a machine learning model for river bed load. *Earth Surf. Dyn.* 11, 681–693.
- Huang, C.-C., Chang, M.-J., Lin, G.-F., Wu, M.-C., Wang, P.-H., 2021. Real-time forecasting of suspended sediment concentrations in reservoirs by the optimal integration of multiple machine learning techniques. *J. Hydrol. Reg. Stud.* 34, 100804.
- 600 Hunziker, R.P., Jaeggi, M.N.R., 2002. Grain sorting processes. *J. Hydraul. Eng.* 128, 1060–1068.
- Kabir, S., Patidar, S., Xia, X., Liang, Q., Neal, J., Pender, G., 2020. A deep convolutional neural

- network model for rapid prediction of fluvial flood inundation. *J. Hydrol.* 590, 125481.
- Karim, F., Armin, M.A., Ahmedt-Aristizabal, D., Tychsen-Smith, L., Petersson, L., 2023. A review of hydrodynamic and machine learning approaches for flood inundation modeling. *Water* 15, 566.
- 605 Karniadakis, G.E., Kevrekidis, I.G., Lu, L., Perdikaris, P., Wang, S., Yang, L., 2021. Physics-informed machine learning. *Nat. Rev. Phys.* 3, 422–440.
- Kasprak, A., Brasington, J., Hafen, K., Williams, R.D., Wheaton, J.M., 2019. Modelling braided river morphodynamics using a particle travel length framework. *Earth Surf. Dyn.* 7, 247–274.
- 610 Kaveh, K., Kaveh, H., Bui, M.D., Rutschmann, P., 2021. Long short-term memory for predicting daily suspended sediment concentration. *Eng. Comput.* 37, 2013–2027.
- Kingma, D.P., Ba, J., 2015. Adam: A method for stochastic optimization 3rd International Conference on Learning Representations. ICLR 2015-Conference Track Proc. 1.
- Kitsikoudis, V., Sidiropoulos, E., Hrissanthou, V., 2014. Machine learning utilization for bed load transport in gravel-bed rivers. *Water Resour. Manag.* 28, 3727–3743.
- 615 Kratzert, F., Klotz, D., Brenner, C., Schulz, K., Herrnegger, M., 2018. Rainfall–runoff modelling using long short-term memory (LSTM) networks. *Hydrol. Earth Syst. Sci.* 22, 6005–6022.
- Kwon, S., Shin, J., Seo, I.W., Noh, H., Jung, S.H., You, H., 2022. Measurement of suspended sediment concentration in open channel flows based on hyperspectral imagery from UAVs. *Adv. Water Resour.* 159, 104076.
- 620 Lesser, G.R., Roelvink, J.A. v, van Kester, J.A.T.M., Stelling, G.S., 2004. Development and validation of a three-dimensional morphological model. *Coast. Eng.* 51, 883–915.
- Ma, M., Zhao, G., He, B., Li, Q., Dong, H., Wang, S., Wang, Z., 2021. XGBoost-based method for flash flood risk assessment. *J. Hydrol.* 598, 126382.
- 625 Madhuri, R., Sistla, S., Srinivasa Raju, K., 2021. Application of machine learning algorithms for flood susceptibility assessment and risk management. *J. Water Clim. Chang.* 12, 2608–2623.
- Mananoma, T., 2009. The effect of sediment supply to the damage of infrastructures. *Eff. Sediment Supply to Damage Infrastructures* 1–489.
- McDonald, R.R., Nelson, J.M., Fosness, R.L., Nelson, P.O., 2016. Field scale test of multi-dimensional flow and morphodynamic simulations used for restoration design analysis.
- 630 Mehedi, M.A. Al, Smith, V., Hosseiny, H., Jiao, X., 2022. Unraveling the complexities of urban fluvial flood hydraulics through AI. *Sci. Rep.* 12, 18738.
- Mentaschi, L., Besio, G., Cassola, F., Mazzino, A., 2013. Problems in RMSE-based wave model validations. *Ocean Model.* 72, 53–58.
- 635 Mohamad, T.H., Abbasi, A., Kim, E., Nataraj, C., 2021. Application of deep cnn-lstm network to gear fault diagnostics, in: 2021 IEEE International Conference on Prognostics and Health Management (ICPHM). IEEE, pp. 1–6.
- Morgan, J.A., Kumar, N., Horner-Devine, A.R., Ahrendt, S., Istanbuloglu, E., Bandaragoda, C., 2020. The use of a morphological acceleration factor in the simulation of large-scale fluvial morphodynamics. *Geomorphology* 356, 107088.

- 640 Ouellet-Proulx, S., St-Hilaire, A., Courtenay, S.C., Haralampides, K.A., 2016. Estimation of suspended sediment concentration in the Saint John River using rating curves and a machine learning approach. *Hydrol. Sci. J.* 61, 1847–1860.
- PyTorch, 2024. ReduceLROnPlateau: PyTorch 2.3 documentation URL: https://pytorch.org/docs/stable/generated/torch.optim.lr_scheduler.ReduceLROnPlateau.html [accessed: May 2024].
- 645 Sahraei, S., Alizadeh, M.R., Talebbeydokhti, N., Dehghani, M., 2018. Bed material load estimation in channels using machine learning and meta-heuristic methods. *J. Hydroinformatics* 20, 100–116.
- Stigler, S.M., 1990. *The history of statistics: The measurement of uncertainty before 1900*. Harvard University Press.
- 650 Talukdar, S., Mankotia, S., Shamimuzzaman, M., Shahfahad, Mahato, S., 2021. Wetland-inundated area modeling and monitoring using supervised and machine learning classifiers. *Adv. Remote Sens. Nat. Resour. Monit.* 346–365.
- USACE, 2021. *HEC-RAS Two-Dimensional Sediment Transport Technical Reference Manual*.
- USGS, 2018. *NED 1/3 arc-second n38w099 1 x 1 degree IMG 2018*: U.S. Geological Survey.
- 655 Veall, M.R., Zimmermann, K.F., 1996. Pseudo-R2 measures for some common limited dependent variable models. *J. Econ. Surv.* 10, 241–259.
- Vercruyssen, K., Grabowski, R.C., Rickson, R.J., 2017. Suspended sediment transport dynamics in rivers: Multi-scale drivers of temporal variation. *Earth-Science Rev.* 166, 38–52.
- 660 Wheaton, J.M., Bouwes, N., Mchugh, P., Saunders, C., Bangen, S., Bailey, P., Nahorniak, M., Wall, E., Jordan, C., 2018. Upscaling site-scale ecohydraulic models to inform salmonid population-level life cycle modeling and restoration actions—Lessons from the Columbia River Basin. *Earth Surf. Process. Landforms* 43, 21–44.
- Williams, R.D., Brasington, J., Hicks, D.M., 2016. Numerical modelling of braided river morphodynamics: Review and future challenges. *Geogr. Compass* 10, 102–127.
- 665 Wu, W., Lin, Q., 2014. Nonuniform sediment transport under non-breaking waves and currents. *Coast. Eng.* 90, 1–11.
- Wu, W., Wang, S.S.Y., Jia, Y., 2000. Nonuniform sediment transport in alluvial rivers. *J. Hydraul. Res.* 38, 427–434.
- 670 Yu, Y., Si, X., Hu, C., Zhang, J., 2019. A review of recurrent neural networks: LSTM cells and network architectures. *Neural Comput.* 31, 1235–1270.
- Zakipour, M., Yazdandoost, F., Alizad, K., Izadi, A., Farhangmehr, A., 2023. An Integrated Resilient Sediment Transport Risk Management (IRSTRIM) Approach for Estuaries. *J. Mar. Sci. Eng.* 11, 1471.
- 675 Zounemat-Kermani, M., Fadaee, M., Adarsh, S., Hinkelmann, R., 2020. Predicting Sediment transport in sewers using integrative harmony search-ANN model and factor analysis, in: *IOP Conference Series: Earth and Environmental Science*. IOP Publishing, p. 12004.